DNS OF TURBULENT CONVECTIVE FLOW BOILING IN A CHANNEL

D. Métrailler, S. Reboux, D. Caviezel and D. Lakehal
ASCOMP, Zurich, Technoparkstr. 1, Switzerland
Metrailler@ascomp.ch; Reboux@ascomp.ch; Lakehal@ascomp.ch

ABSTRACT

Heat transfer in PWRs' sub-channels results from a complex interplay between nucleate boiling, turbulence and interfacial flow, each of which individually represents a challenge to resolve numerically. This motivates the development of accurate numerical tools for the analysis of convective flow boiling. This paper presents results of a Direct Numerical Simulation (DNS) of subcooled water flowing in a channel at Re_τ=400 using the code TransAT. Part of the channel is heated with a constant heat flux, in the same setup as in the experiment of B. Phillips, J. Buongiorno and T. McKrell (*NURETH-15,* 2013) [1].
The computational results are in good agreement with the experimental measurements, although the simulation tends to over-predict coalescence events and under-predict condensation rate. The resulting DNS flow database can be used to provide up-scaled closure models in mixture simulations and to assess the single-phase vs. multiphase flow convection heat transfer coefficient.

KEYWORDS
Interface Tracking, turbulence, convective boiling, LES, DNS

1. INTRODUCTION

The prediction of critical heat flux (CHF) conditions is vital in many industrial systems. In pressurized nuclear power reactors, CHF is a kind of limit parameter of operation, therefore its accurate prediction is important both from safety and economic point of views. In the last decade, considerable efforts have been made to use computational fluid dynamics (CFD) methods for the prediction of CHF. The limited success of these attempts motivates more work on the side of modeling. To support the modeling efforts we need reliable and accurate measurements, which are dedicated for development and validation of CFD methods. Beside complex CHF measurements, separate effect tests can be used to develop particulate models relevant in complex CHF modeling. In the development of CHF all transport mechanisms such as mass, momentum and energy transfer play important role.
In the PWR hot channel, beyond the onset of nucleate boiling but before the point of net vapor generation, small vapor bubbles are attached to the fuel rods. Heat and mass are transferred by evaporation from the base to the tip of the bubbles where condensation occurs; therefore, the heat transfer coefficient increases with respect to single-phase flow conditions. Also, the bubbles, effectively, act as surface roughness and thus, depending on their size, may affect the friction coefficient and ultimately the flow distribution across the sub-channels within the fuel assembly.
The detailed analysis of the interactions between near-wall (seeded) bubbles and turbulence is presented in a companion paper (these Proceedings). This work focuses on the heat transfer mechanisms at play during bubble nucleation, as the same turbulent flow is heated by a plate above saturation temperature.
Analytical solutions exist for heat transfer in laminar and single-phase flows, but few data are available in the complex case of turbulent nucleated bubbles. The challenges are multiple: The physical models required to correctly capture the phase-change and turbulence mechanisms are complex and intrinsically coupled. Even though subgrid models are used to account for effects at the smallest scales, the computational resources needed remain huge (up to 1'200 processors were used in parallel).
In the present study a 10 degrees subcooled turbulent flow (Re_τ = 400) is heated by a plate with constant heat transfer (q''_w = 500 kW/m^2). Furthermore the simulation is able to automatically nucleate small-scale

bubbles. The phase change between the nucleated bubbles and the main flow is also modeled. This simulation is a first attempt to evaluate the proportion and scales of the three heat fluxes commonly defined in nucleate boiling cases: single phase, phase change and quenching heat flux. Some elements are not taken into account in the simulation. For example, other aspects such as roughness, hydrophilicity and porosity of the heater are not modeled. These simulations aim to partially reproduce Philips, McKrell & Buongiorno's experiment [1]. The schematic of the experimental setup is shown in Figure 1.

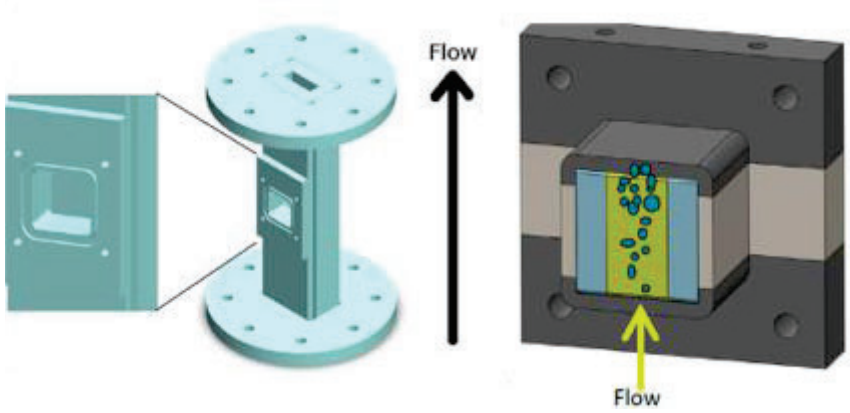

Figure 1: Experimental setup for HSV and IR thermography (left), picture of the quartz section (middle), and diagram of flow channel with the heated area shown in red. [1]

High-Speed Video (HSV) and Infrared (IR) thermography were used to report bubble departure diameter, and IR thermography allowed measurement of wall superheat (local distribution and surface-averaged), heat transfer coefficient, nucleation site density, and bubble wait time. The tests were performed at atmospheric pressure at a constant sub-cooling of 10º C.

2. PROBLEM SETUP

The flow is initialized from the single-phase water flow at Re_τ=400 generated for a companion paper. The domain size and discretization are identical. For the sake of clarity, the mesh and boundary conditions are shortly recalled. Special precaution is dedicated to the turbulence sustainability. The nucleation and condensation models are also introduced. Finally the first results of the single-phase heat transfer and convective boiling flow are presented. Large discussion is given on the improvement possibilities and extension of this work.

2.1Domain size and discretization

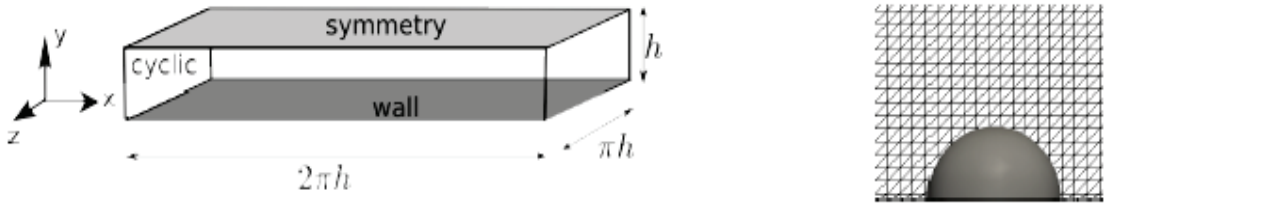

(a) Size of the computational domain and boundary conditions.

(b) A bubble with diameter D_b imposes that $\Delta x = D_b/8$.

Figure 2: Computational domain.

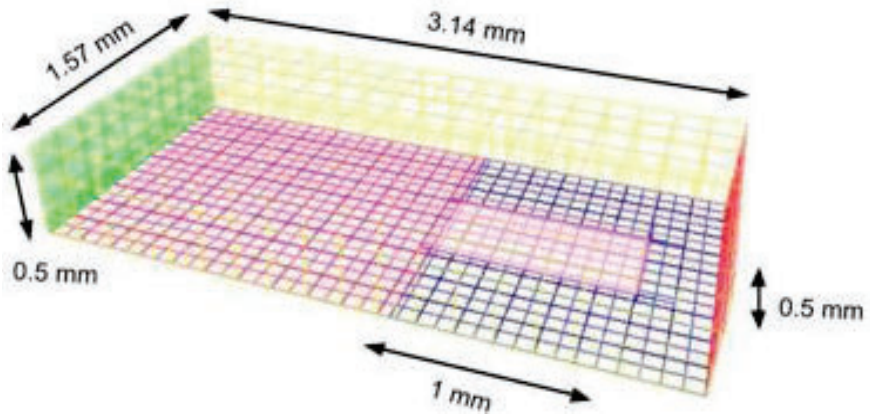

Figure 3: Boundary conditions.

The physical channel has a length of 2πh, a height of 2h and width of h. The y-coordinate is the wall-normal coordinate. The heater has an area of 0.005 cm^2. The flow is assumed to be at atmospheric pressure and with a sub-cooling of 10 [K]. The friction Reynolds number is Re_τ=400, corresponding to a mass flux of 1.250 [kg/s/m2]. The bubble radius r_b is chosen to be 0.125 mm, which corresponds to the departure size observed in the experimental conditions. To be consistent with the work of Chatzikyriakou et al. [2, 3] the normalized bubble radius $k^+=u_\tau/\nu\ r_b$ is chosen to be equal to 10. Using interface tracking for the dispersed phase requires a relatively fine mesh in all directions. A grid spacing of 8 cells for one bubble diameter was found to be sufficient, yielding the normalized grid spacing:$\Delta h_f^+ = \Delta x_f^+ = \Delta y_f^+ = \Delta z_f^+ = 2.5$. A block mesh refinement (BMR) technique is used to coarsen the grid by a factor 2 away from the wall (for y^+ larger than 90). This leads to approximately 30 million grid cells, distributed in 1'134 blocks. The load balancing is satisfactory, with each block having between 20'000 and 25'000 cubical-shaped cells. The first grid point is at y^+ = 1, which is inside the viscous sublayer.

2.2Boundary conditions

A symmetry boundary condition was used at half channel height to reduce computational effort. Periodic boundary conditions were used in the streamwise and spanwise directions. A constant pressure is imposed at the domain outlet. The presence of the heater prevents the use of periodic boundary conditions in the flow direction; a virtual plane was thus immersed in the region upstream of the heater. The values captured on this plane are used as inflow boundary conditions for the inlet. Thus the flow is recycled and constant mass flow rate is guaranteed, which sustains a developed turbulence flow past the heater plate.

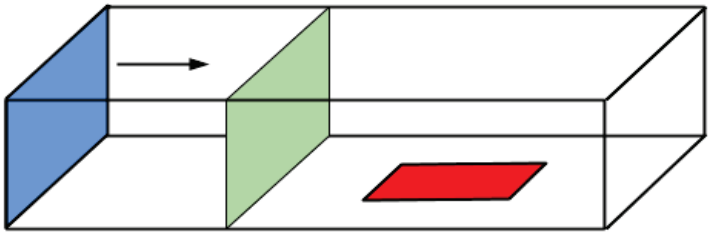

Figure 4: Turbulence recirculation. Green: virtual plane; blue: inlet; red: heater.

3. MODELING

TransAT©, which has been used here, is a multi-scale, multi-physics, conservative finite-volume solver for single- and multi-fluid Navier-Stokes equations. The discretization algorithms and schemes employed for pressure-velocity coupling are all high order. In LES the motion of the supergrid turbulent eddies is directly captured, whereas the effect of the smaller scale eddies is modeled. In terms of computational cost, LES [4] lies between RANS and DNS and is motivated by the limitations of each of these approaches. Since the large-scale unsteady motions are represented explicitly, LES is more accurate and reliable than RANS. In this work, the subgrid scales were modeled using the wall-adapting local eddy-viscosity (WALE) model. The same value of Cs=0.08 as in [2] was used. Interface tracking was performed using the Level-Set method, with an implicit time-stepping scheme and WENO re-initialization. The phase change mechanisms need to be modeled. In TransAT the level set method can be used with multiple phase change models. The direct phase change method and the wall nucleation model are hereby presented.

3.1Condensation-Evaporation

The level set advection equation is extended with a source term on the right hand side. The mass transfer term is activated only at the interface and is directly related to the temperature difference $T-T_{sat}$ where T_{sat} is the saturation temperature.

$$\frac{\partial \phi}{\partial t} + u_j \frac{\partial \phi}{\partial x_j} = -\frac{\rho}{\rho_l}\frac{\dot{m}}{\rho_g}\left|\frac{\partial \phi}{\partial x_j}\right|; \qquad \dot{m} = \frac{2\lambda(T - T_{sat})\delta(\phi)}{L}$$

3.2Boiling SGS model

TransAT has a built-in model to capture nucleation events in flows over heated surfaces. It assumes that phase-change occurs instantly as soon as the local temperature exceeds saturation temperature. A subgrid-scale (SGS) model is used to provide accurate spatial discretization near the walls.
The SGS front is initiated when the temperature of one of the near wall cells is larger than the saturation temperature. It then evolves according to the energy flux balance, accounting for influx of heat from the wall and the latent heat of the fluid.

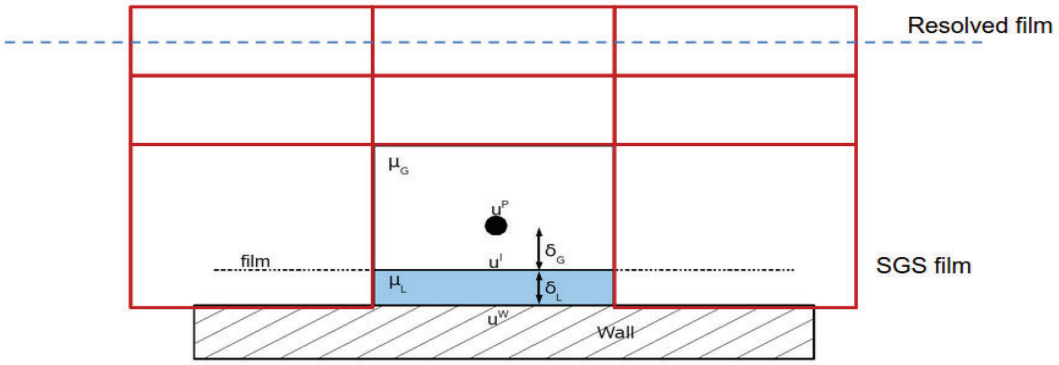

Figure 5: Boiling SGS model.

3.3Validation

This approach was validated by comparing the evolution of a film described by a level-set on a very fine mesh with a film described by the SGS model on a coarser mesh. The temperature of the wall was 5 degrees above saturation temperature in both cases. The results are very similar, as shown in Figs. 6 & 7.

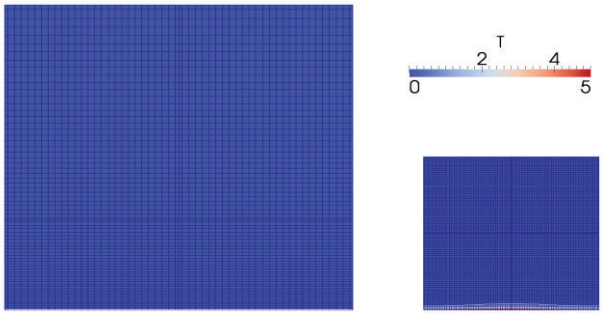

Figure 6: Initial conditions. Left: SGS model; right: prescribed LS film

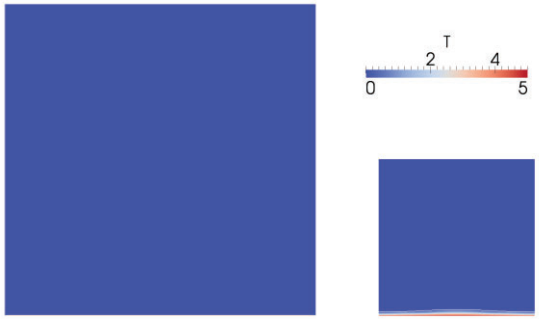

t = t0. Left: SGS; right: LS

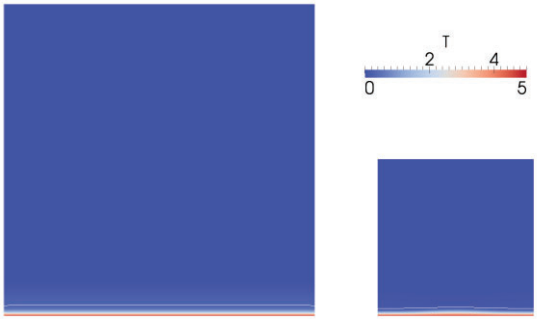

t = t1. Left: SGS; right: LS

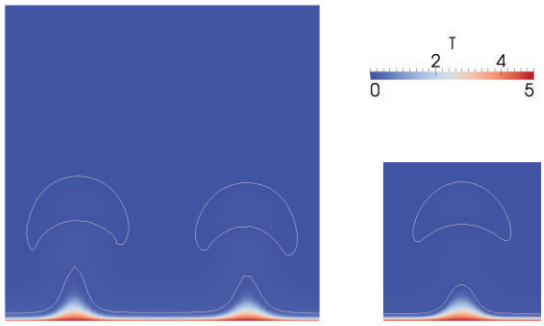

t = t2. Left: SGS; right: LS

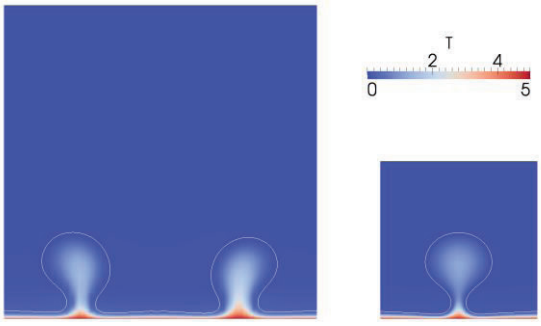

t = t3. Left: SGS; right: LS

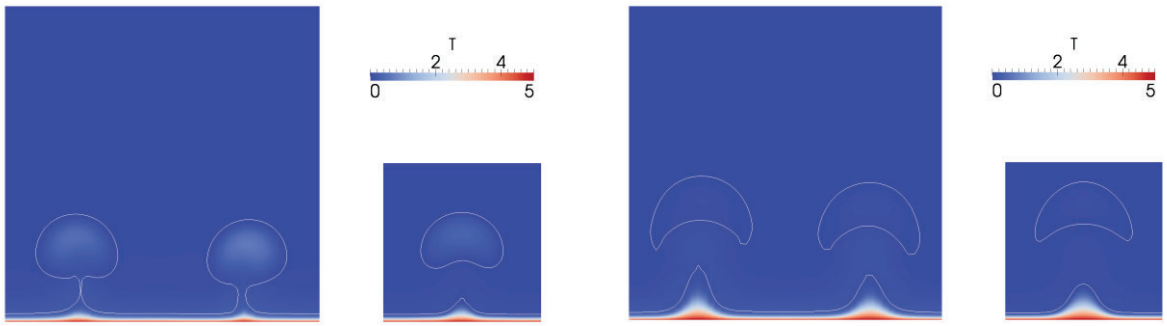

t = t4. Left: SGS; right: LS

t = t5. Left: SGS; right: LS

Figure 7: Evolution of nucleated bubbles, comparison between SGS model and Level-Set film initial conditions

4. SIMULATION RESULTS

4.1 Convective single-phase heat transfer

At first, a single-phase turbulent flow is simulated on a heated plate. In this simulation, phase change is not taken into account and no bubbles are present. The heater generates a heat flux of 500 kW/m^2. The inflow is subcooled at 10 [K].

Figure 8 shows a horizontal slice through the domain at y=0.1 mm. The temperature and u-velocity distribution are compared. The velocity streaks of the turbulent flow are directly related to the temperature streaks on the heater. As suspected the regions with low velocities exhibit large temperatures, and vice versa.

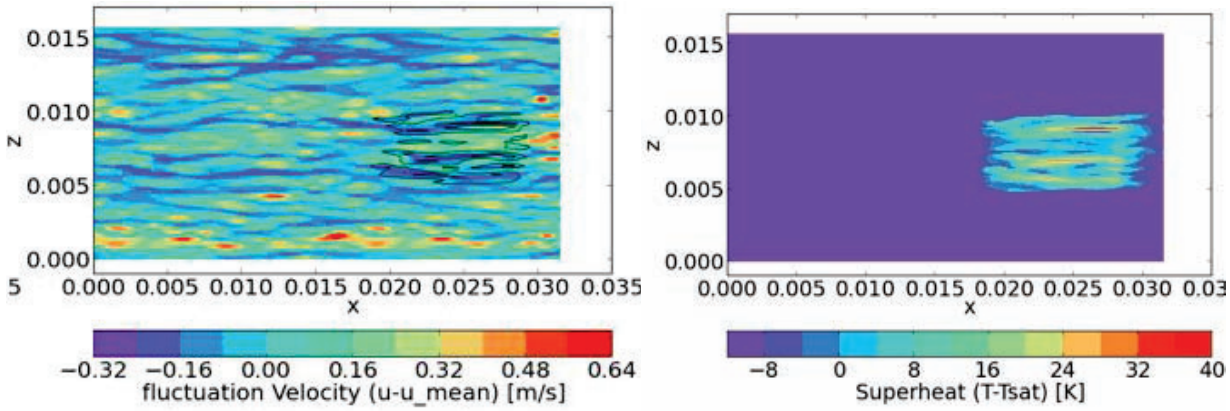

Figure 8: Velocity and temperatures at y=0.1 mm.

These results are first indications of the location of the nucleation site. We therefore expect bubbles to appear in region being affected by slow velocities.

4.2 Convective boiling flow

In this simulation, the boiling subgrid scale model is enabled and phase change is enabled. Bubbles can therefore be automatically created on the wall where $T > T_{sat}$. Streamlines, velocity and temperature slices in normal to the wall and the flow direction are shown in Figures 9-11.

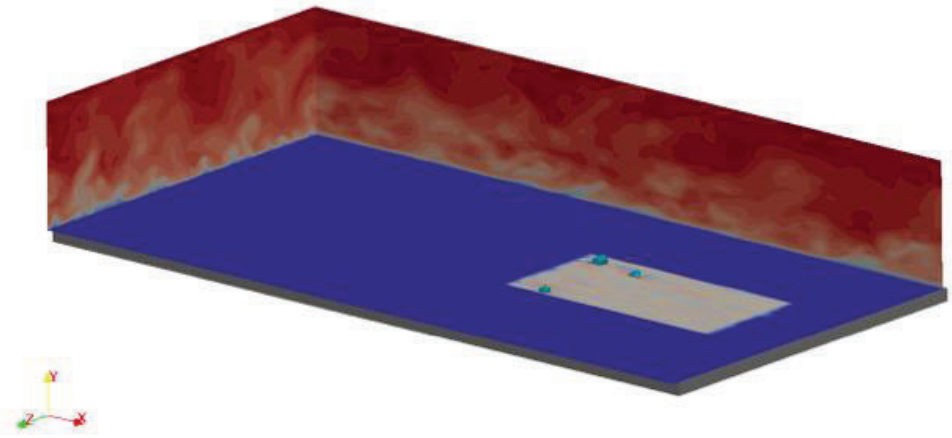

Figure 9: First bubbles on the heater. The heater is colored by temperature; the side panels show the longitudinal velocity.

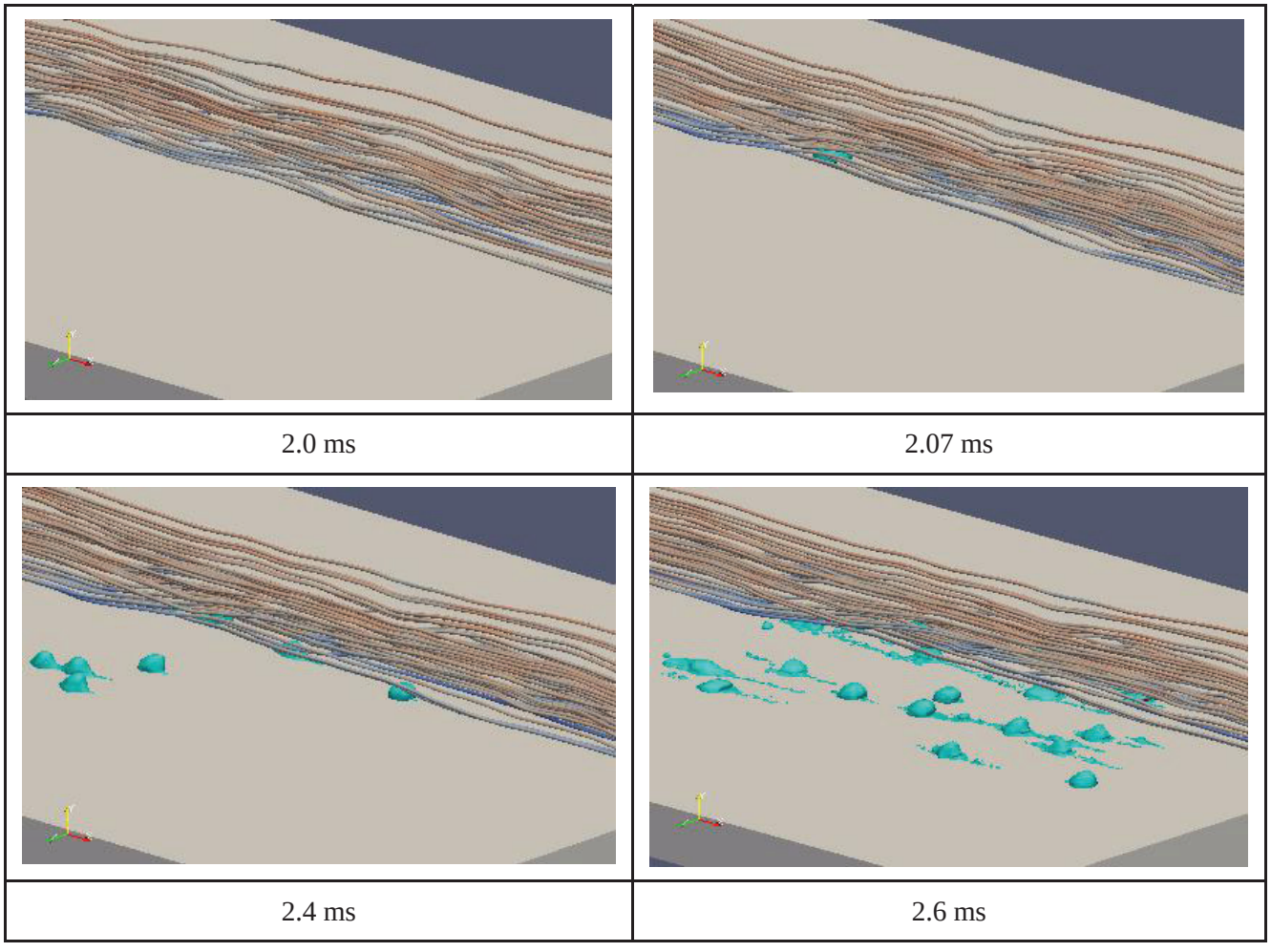

Figure 10: Vapor bubbles and streamlines colored by velocity magnitude.

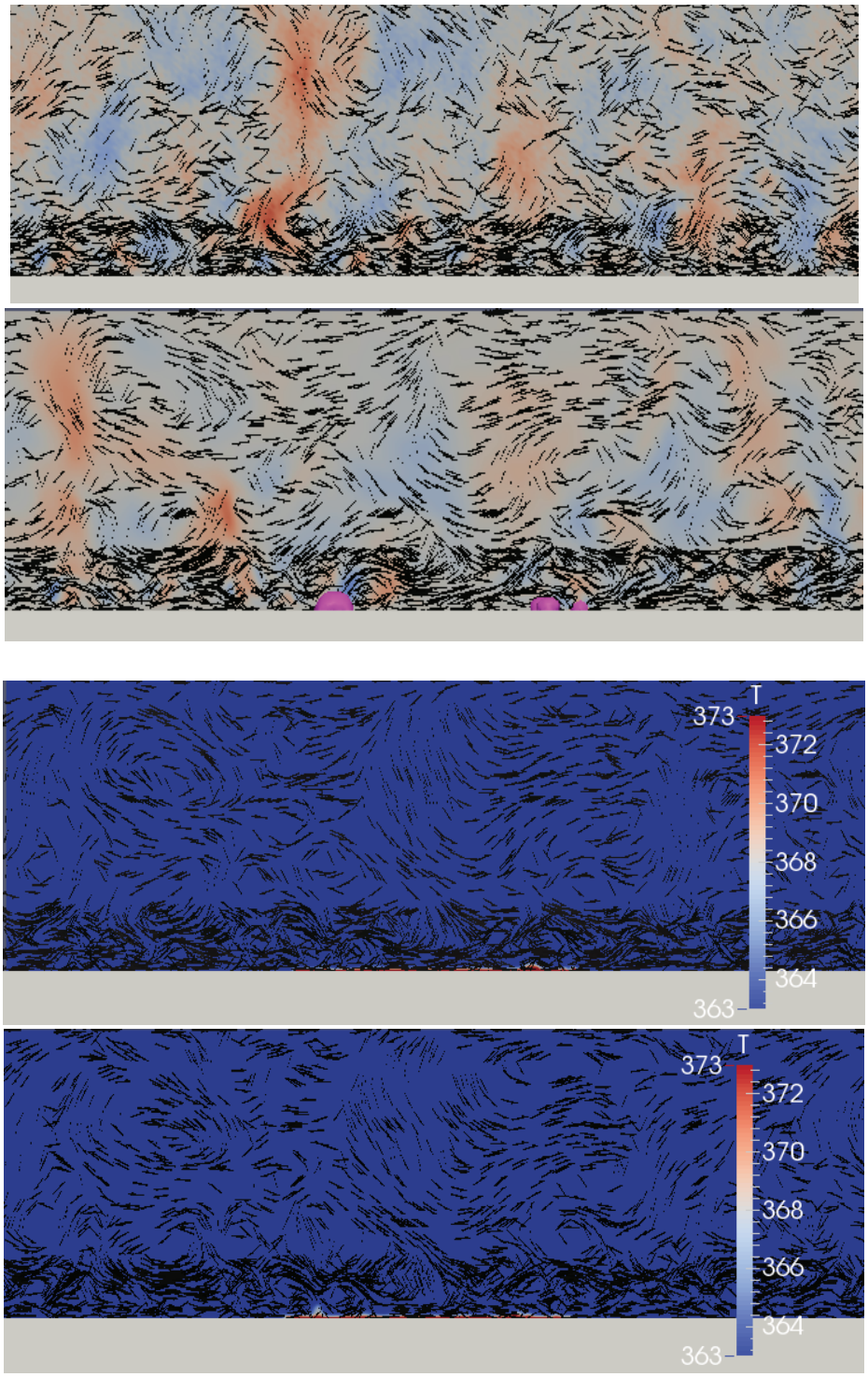

Figure 11: Velocity field intensities and temperature profiles

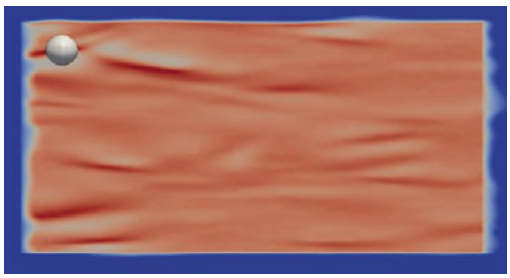	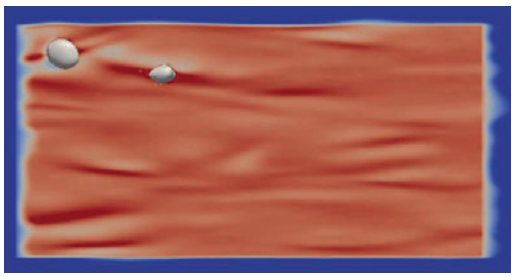
1 bubble timestep = 1000, time = 2.0708 [ms]	2 bubbles timestep = 1600, time = 2.2071 [ms]
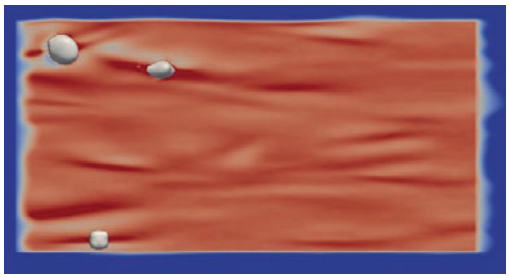	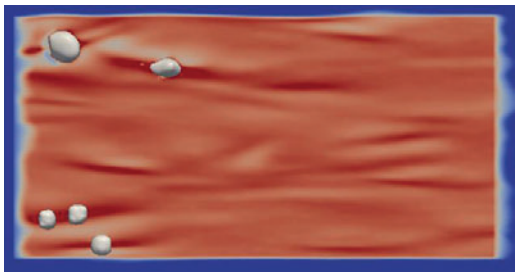
3 bubbles timestep = 1900, time = 2.3002 [ms]	4 and 5 bubbles timestep = 2000, time = 2.3303 [ms]

Figure 12: Bubbles nucleation with temperature slice.

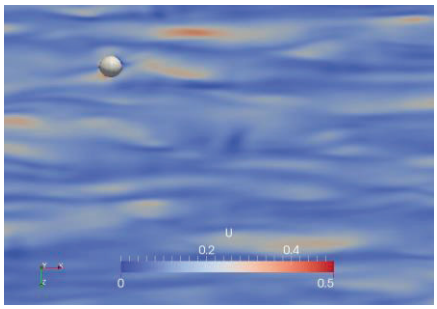	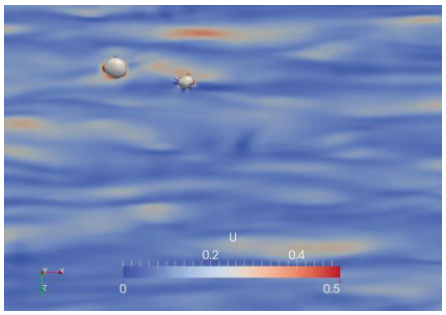
1 bubble, time = 2.0708 [ms]	2 bubbles, time = 2.2071 [ms]
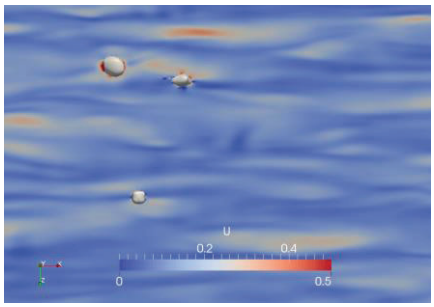	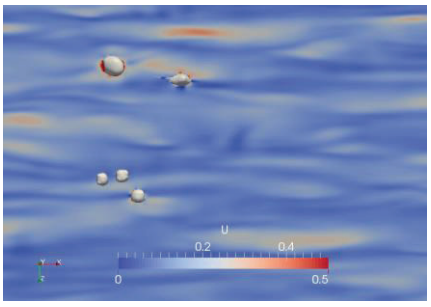
3 bubbles, time = 2.3002 [ms]	4 and 5 bubbles, time = 2.3303 [ms]

Figure 13: Bubbles nucleation with velocity slice.

5. CONCLUSION

This paper presents results of a Direct Numerical Simulation (DNS) of subcooled water flowing in a channel at Re_τ=400 using the CFD code TransAT. Part of the channel is heated with a constant heat flux, in the same setup as in the experiment of [1]. Bubble dynamics are resolved using a Level Set interface tracking method. It is combined with a subgrid model able to capture nucleation at the wall where the local temperature exceeds the saturation temperature. Fully developed turbulence is maintained upstream of the heated region using cyclic boundary conditions. Vapor bubbles grow, coalesce and condense into the subcooled liquid, affecting the wall-layer turbulence. Gaseous patches are formed in locations that correlate with thermal wall streaks in the streamwise direction. Cross-flow structures are also shown to have an impact on the rate of heat removal.

The computational results are in good agreement with the experimental measurements, although the simulation tends to over-predict coalescence events and under-predict condensation rate. The resulting DNS flow database can be used to provide up-scaled closure models in mixture simulations and to assess the single-phase vs. multiphase flow convection heat transfer coefficient.

The above analysis is valid for a small time scale focusing on the first nucleated bubbles. For longer time scales the simulated flow transitions to film boiling, although this is clearly not the case in the experimental conditions of Philips et al. This can be explained by the type of boundary conditions chosen in our simulations. We assumed a constant heat flux, independently of the phase in contact with the heater. The vapor temperature close to the wall thus becomes much larger than the saturation temperature. This artifact would not occur with more realistic boundary conditions that include the conjugate heat transfer between the fluid and the heated solid substrate. That is the subject of ongoing work.

6. ACKNOWLEDGMENT

This work has been accomplished in the frame of the FP7 project NURESAFE under grant agreement no 323263. ASCOMP acknowledges PRACE for awarding access to resource Hermit based in Germany at HLRS.

7. REFERENCES

[1] B. Phillips, J. Buongiorno and T. McKrell. ‘Nucleation site density, bubble departure diameter, wait time and local temperature distribution in subcooled flow boiling of water at atmospheric pressure, as measured by synchronized high-speed video and infrared thermography’, Proceedings NURETH 15, Pisa, May 12-15 (2013)

[2] D. Chatzikyriakou, J. Buongiorno, D. Lakehal. ‘Benchmarks for interface tracking codes in the Consortium for Advanced Simulation of LWRs (CASL)’, NURETH-14, Toronto, Sept. 25-29, (2011)

[3] D. Chatzikyriakou, J. Buongiorno, D. Caviezel, D. Lakehal. ‘DNS and LES of turbulent flow in a closed channel featuring a pattern of hemispherical roughness elements’, International Journal of Heat and Fluid Flow 53, 29–43 (2015)

[4] P. Sagaut. ‘Large Eddy Simulation for Incompressible Flows’, Springer Verlag (2006)